Published in final edited form as:

*J Cell Physiol*. 2024 January ; 239(1): 36–50. doi:10.1002/jcp.31142.

# Salmonella engages CDC42 effector protein 1 for intracellular invasion

**Sheila Bandyopadhyay**[1], **Xiao Zhang**[1], **Andrea Ascura**[1], **Karen L. Edelblum**[2], **Edward M. Bonder**[1], **Nan Gao**[1]

[1]Department of Biological Sciences, Rutgers University, Newark, New Jersey, USA

[2]Department of Pathology, Immunology, and Laboratory Medicine, Center for Immunity and Inflammation, Rutgers New Jersey Medical School, Newark, New Jersey, USA

## Abstract

Human enterocytes are primary targets of infection by invasive bacterium *Salmonella* Typhimurium, and studies using nonintestinal epithelial cells established that *S*. Typhimurium activates Rho family GTPases, primarily CDC42, to modulate the actin cytoskeletal network for invasion. The host intracellular protein network that engages CDC42 and influences the pathogen's invasive capacity are relatively unclear. Here, proteomic analyses of canonical and variant CDC42 interactomes identified a poorly characterized CDC42 interacting protein, CDC42EP1, whose intracellular localization is rapidly redistributed and aggregated around the invading bacteria. CDC42EP1 associates with SEPTIN-7 and Villin, and its relocalization and bacterial engagement depend on host CDC42 and *S*. Typhimurium's capability of activating CDC42. Unlike CDC42, CDC42EP1 is not required for *S*. Typhimurium's initial cellular entry but is found to associate with *Salmonella*-containing vacuoles after long-term infections, indicating a contribution to the pathogen's intracellular growth and replication. These results uncover a new host regulator of enteric *Salmonella* infections, which may be targeted to restrict bacterial load at the primary site of infection to prevent systemic spread.

### Keywords

bacterial invasion; cdc42; cdc42ep1; intracellular bacteria; salmonella

## 1 | INTRODUCTION

*Salmonella enterica* serovar Typhimurium (*S*. Typhimurium) is a Gram-negative enteropathogenic bacterium that causes 90 million cases of human illness each year and

**Correspondence** Nan Gao, Department of Biological Sciences, Rutgers University, 195 University Ave, Boyden Hall Suite 206, Newark, NJ 07102, USA. ngao@newark.rutgers.edu.

AUTHOR CONTRIBUTIONS

Sheila Bandyopadhyay, Nan Gao, and Edward M. Bonder contributed to the study conception and design. Sheila Bandyopadhyay, Xiao Zhang, and Andrea Ascura contributed to experimental execution and data acquisition. Sheila Bandyopadhyay was responsible for all formal data analysis and visualization. Nan Gao and Karen L. Edelblum were responsible for providing experimental resources. Sheila Bandyopadhyay, Nan Gao, and Edward M. Bonder contributed to the manuscript preparation and manuscript editing.

SUPPORTING INFORMATION

Additional supporting information can be found online in the Supporting Information section at the end of this article.

can become lethal in patients with compromised immunity (Eng et al., 2015; Martin et al., 2004). The bacteria induce diarrhea and gastroenteritis as a result of the host inflammatory response and disruption of intestinal epithelial barrier integrity (Boyle et al., 2006). *S.* Typhimurium utilize their virulence effectors to invade host cells, replicate intracellularly, and spread to other tissues (Galán, 2001). Genes encoded by the *Salmonella* pathogenicity island–1 (SPI-1) facilitate the bacterial invasion into intestinal epithelial cells (IECs) (Kubori & Galán, 2003; Kubori et al., 2000; Que et al., 2013), while SPI-2 is responsible for the intracellular maturation of *Salmonella*-containing vacuoles (SCVs) and successful colonization of the host (Figueira & Holden, 2012; Hansen-Wester & Hensel, 2001). *S.* Typhimurium form SCVs to survive and replicate within the host cells. SCVs are found to be enriched with early endocytic markers EEA1 and RAB5 in the initial phase of invasion and are decorated with lysosome-associated membrane proteins (LAMPs) and vATPases later in the infection cycle (Beuzon, 2000; Steele-Mortimer et al., 1999; Steele-Mortimer, 2008). How *Salmonella* engages host protein machinery and assembles SCVs is still not fully understood.

To invade nonphagocytic IECs, *S.* Typhimurium induce rapid and extensive host cytoskeletal modifications (Patel & Galán, 2005). These responses are elicited by bacterial virulence factors injected through a needle-like structure, which is a component of the type III secretion system (T3SS) (Kubori et al., 2000). Among these virulence factors, SopB, SopE, and SopE2 activate the host cell Rho GTPases (Boyle et al., 2006; Hardt et al., 1998; Zhou et al., 2001), SipA and SipC nucleate and bundle actin (Hayward & Koronakiss, 2002; Hayward, 1999; Zhou et al., 1999), and SptP deactivates Rho GTPases after bacterial internalization (Fu & Galán, 1999; Murli et al., 2001). These studies suggest that actin rearrangements are required for bacterial internalization. For instance, treating MDCK epithelial cells with cytochalasin D, an actin polymerization inhibitor, prevented *S.* Typhimurium uptake (Finlay et al., 1991). However, actin inhibitors exhibit toxicity and a wide spectrum of consequences on cellular physiology (Cooper, 1987; Moon et al., 2008; Richter et al., 2021; Usui et al., 2004).

CDC42 belongs to the Rho GTPase family, regulates actin cytoskeleton reorganization, and is a major host cell protein required for *S.* Typhimurium invasion (Brown et al., 2007; Chen et al., 1996; Nobes & Hall, 1995). SopE and SptP act as a guanine-nucleotide exchange factor (GEF) and a GTPase-activating protein (GAP), respectively, for CDC42 (Fu & Galán, 1999; Kubori & Galán, 2003). A dominant negative mutant CDC42 decreased the invasive ability of the bacteria in COS-1 cells (Chen et al., 1996), while inhibition of CDC42 prenylation also inhibited Salmonella-induced disruption of an MDCK-1 cell monolayer (Tafazoli et al., 2003), suggesting that intracellular localization of the CDC42 machinery may be essential for bacterial entry. However, human enterocytes are the primary targets of Salmonella infection, and little is known about the protein complex of CDC42 machinery that engages and regulates *Salmonella* invasion in this cell type.

Here, CDC42 proteomic analyses revealed the poorly characterized Cdc42/Rac interactive binding motif (CRIB)-domain-containing CDC42 Effector Protein 1 (CDC42EP1) (Hirsch et al., 2001), which showed strong interactions with both the canonical and splice variant forms of CDC42. CDC42EP1 is abundant in (IECs) and increased by the colonization of

epithelium-attaching commensal bacteria in mice (Ladinsky et al., 2019). Other than the potential involvement of CDC42EP1 in the migration of mouse embryonic stem cells and cardiac endothelial cells (Liu et al., 2014; Vong et al., 2010), knowledge of CDC42EP1's function in general is limited, and no study has implicated its role during infection. Using a polarized human enterocyte culture model, we demonstrate that invading *S.* Typhimurium rapidly engages with CDC42EP1 for intracellular invasion and replication.

## 2 | RESULTS

### 2.1 | CDC42EP1–CDC42 interaction is regulated by CDC42 activation and lipidation

Mammalian CDC42 has two alternative splicing variants, the canonical CDC42-V1 and the variant CDC42-V2, which differ in the last 10 amino acids (Kang et al., 2008; Nishimura & Linder, 2013; Wirth et al., 2013; Yap et al., 2016). Since both CDC42 variants are physiologically expressed, we performed proteomics analysis of 3xFLAG-tagged CDC42-V1 and CDC42-V2 which were transiently transfected into HEK293T cells, immunoprecipitated, and the products were analyzed by mass spectrometry (Zhang et al., 2020). Within both CDC42 variant proteomes, CDC42EP1 was found (Supporting Information: Table 1). Search Tool for the Retrieval of Interacting Genes/Proteins (STRING) analysis was performed using unsupervised clustering of actin-associated proteins found within the CDC42 interactomes. The results suggested that CDC42 and CDC42EP1 may cooperate during Arp2/3 complex-mediated actin nucleation and Rho protein signal transduction (Figure 1a,b). Using coimmunoprecipitation (co-IP) assays, we verified CDC42EP1 interactions with 3xFLAG-CDC42-V1 and 3xFLAG-CDC42-V2 (Figure 1c). The results also suggested similar levels of interaction between CDC42EP1 and both CDC42 variants (Figure 1c). Immunostaining for endogenous CDC42EP1 in both HeLa and HEK293T epithelial cell lines revealed a diffuse staining pattern, with increased intensities at cellular junctions in the confluent HEK293T monolayer (Supporting Information: Figure 1).

Most CDC42 effectors bind to CDC42 that is in a guanosine triphosphate (GTP)-bound active conformation (Haspel et al., 2021; Leung & Rosen, 2005; Sinha & Yang, 2008). To determine whether the activity of CDC42 affects its ability to interact with CDC42EP1, we tested the interaction of CDC42EP1 with a 3xFLAG-tagged fast cycling mutant CDC42-V1 (F28L), which has increased guanosine diphosphate (GDP)/GTP exchange activities (Lin et al., 2003). Co-IP assay demonstrated a strong interaction between CDC42EP1 and CDC42-V1-F28L (Figure 1d). Likewise, we performed similar experiments to test CDC42EP1 binding to a constitutively active CDC42-V2-G12V and a dominant negative CDC42-V2-T17N. Co-IP analysis showed that CDC42EP1 was associated with wild-type and the constitutively active CDC42 forms, but demonstrated a significantly reduced association with the dominant negative isoform (Figure 1e). These data suggest that CDC42EP1 primarily interacts with active forms of CDC42.

CDC42-V2 differs from the canonical CDC42-V1 by only the last 10 amino acids at the C-terminus (Marks & Kwiatkowski, 1996; Nishimura & Linder, 2013; Wirth et al., 2013). While CDC42-V1 possesses a CaaX motif that can undergo a prenylation modification, CDC42-V2 contains a CCaX motif that can be both prenylated and palmitoylated

(Nishimura & Linder, 2013; Roberts et al., 2008). As lipid modifications alter the subcellular locations of GTPases, we determined, through the use of three lipidation-defective CDC42-V2 mutants (C188A, C189A, and C188/189A), whether lipid modifications of CDC42 affect its interaction with CDC42EP1. Co-IP assays showed that CDC42EP1 failed to interact with C188A and C188/189A mutants in which the C188 prenylation residue was mutated (Figure 1f), but the interaction remained with the C189A palmitoylation mutant. As prenylation modifications typically target proteins to cellular membranes (Gomes et al., 2003), these data suggest that CDC42EP1 may preferentially interact with CDC42 in certain membrane-enclosed intracellular compartments.

### 2.2 | *S.* Typhimurium infection rapidly alters CDC42EP1 localization and interaction with CDC42

The proteomics analyses and clustering of actin-associated proteins within the CDC42 interactome suggested that CDC42EP1 may interact with CDC42 during its regulation of actin remodeling (Figure 1a,b). CDC42EP1 has also been associated with pathogenic colonization (Ladinsky et al., 2019), and therefore, may interact with CDC42 during the actin remodeling that takes place upon invasion by *Salmonella*. To test if CDC42EP1 is an integral part of CDC42 machinery during *S.* Typhimurium invasion (Chen et al., 1996; Rodríguez-Escudero et al., 2011; Stender et al., 2000), we first evaluated CDC42EP1 and CDC42 interaction before and 30 min after an *S.* Typhimurium infection of HEK293T cells. After infection, CDC42EP1 was robustly expressed (Figure 2a), and its association with both CDC42-V1 or CDC42-V2 appeared to increase (Figure 2b). Additionally, in both Caco-2 and C2Bbe1 colonic epithelial cells, transcript levels of CDC42EP1 moderately increased up to 15 min after *S.* Typhimurium infection (Supporting Information: Figure 2a).

We next examined CDC42EP1's intracellular localization in response to *S.* Typhimurium infection. Since *Salmonella* has been reported to induce changes in host cells within 1 min upon exposure (Schlumberger et al., 2005) and to observe dynamic changes upon bacterial entry, we performed infections from 5 min up to 30 min. Before infection, CDC42EP1 was found diffused in the cytoplasm and slightly enriched at the plasma membrane of HeLa cells (Figure 2c). Within 5 min of adding *S.* Typhimurium to the culture, CDC42EP1 demonstrated a more punctate pattern and was found redistributed to regions with intracellular bacteria (Figure 2c).

To investigate if this dramatic CDC42EP1 redistribution occurs in human enterocytes, we performed time-course infection experiments in the C2Bbe-1 cell line, a subclone of human Caco-2 colonic epithelial cells isolated for its apical localization of Villin (Peterson & Mooseker, 1992), an actin-bundling protein. Villin was previously shown to facilitate the entry of *Salmonella* into IECs (Lhocine et al., 2015); therefore, the abundant Villin expression in these highly polarized C2Bbe-1 cells makes them an ideal model for *Salmonella* infection studies. Within 5 min of infection, CDC42EP1 relocalized to specific regions next to invading *S.* Typhimurium in C2Bbe-1 cells (Figure 2d,e), and remained associated with invading bacteria for 15 min and 30 min (Figure 2e,f). Higher resolution microscopy revealed that smaller puncta of CDC42EP1 accumulated around the invading bacteria (Figure 2g). Similar observations were made in the confluent regular Caco-2 cell

line with a consistent temporal change in CDC42EP1 localization. These results suggest that the invading bacteria recruit intracellular CDC42EP1 in both intestinal and nonintestinal cell types.

*S.* Typhimurium assembles SCVs, decorated by endocytic markers such as LAMP-1, after the initial invasion to facilitate their survival and replication within host cells (Beuzon, 2000; Steele-Mortimer et al., 1999). To determine if CDC42EP1 remains associated with intracellular *Salmonella* as the bacteria progress through the infectious cycle, we analyzed LAMP-1 and CDC42EP1 in C2Bbe1 cells after a 30-min infection, a gentamicin wash-out of extracellular bacteria, followed by 4.5-h of intracellular growth. Five hours after the initial exposure to *Salmonella*, CDC42EP1 no longer encircled the bacteria but was found to colocalize with bacteria residing in LAMP1-positive SCVs (Figure 2h). These data suggest that *Salmonella* rapidly and robustly redistribute CDC42EP1 upon initial invasion of host epithelial cells, and a fraction of CDC42EP1 is present on *Salmonella*-associated structures in the later stages of infection (Supporting Information: Figure 2b).

### 2.3 | CDC42EP1 is recruited to an actin-associated ring around invading *S.* typhimurium

Like other invasive pathogens, *S.* Typhimurium rely on extensive host actin remodeling for entry of host cells (Finlay & Falkow, 1990; Finlay et al., 1991; Francis et al., 1993). To determine, in detail, the molecular complex of CDC42EP1 associated with invading *Salmonella*, we stained for CDC42EP1 and actin filaments before and after *S.* Typhimurium infection. In both Caco-2 and C2BBe1 cells, 5 min after the addition of *Salmonella*, CDC42EP1 formed circular aggregates around the invading bacteria, which colocalized with actin ruffling (Figure 3a,b), suggesting that CDC42EP1 was recruited by the bacteria during initial invasion of the cell. The circular CDC42EP1 appeared to aggregate into a "ring"-like structure, ranging from 6.8 to 7.9 μm and surrounding many of the bacteria (2–5 μm on average), which appeared to take a central position inside the surrounding actin and CDC42EP1 (Figure 3c, Supporting Information: Figure 3a, 3b). The average Pearson's correlation coefficient for colocalization of CDC42EP1 and actin around invading bacteria in both cell lines was 0.68 ± 0.13, suggesting a positive relationship between CDC42EP1 and actin enrichment. Nearly all the intracellular bacteria that were surrounded by CDC42EP1 accumulation were also encircled by actin (Figure 3d). In contrast, about 50% of the bacteria that were surrounded by actin ruffling were encircled by CDC42EP1 accumulation (Figure 3d), suggesting that CDC42EP1 recruitment occurs in a subset of these invading bacteria. In those bacteria that were surrounded by both, actin protrusions extend more apically than CDC42EP1 (Figure 3e). These results suggest that *S.* Typhimurium infection induces a spatial and temporal CDC42EP1 relocalization to bacterium-encircling actin filaments.

Although the function of CDC42EP1 and its interplay with CDC42 in enteric pathogen invasion are unknown, CDC42EP1 has been reported to bind SEPTIN family members, GTP-binding cytoskeletal components that form hetero-oligomeric complexes and act as intracellular scaffolds or barriers reported to aid or inhibit bacterial infections (Boddy et al., 2018; Farrugia & Calvo, 2016; Mostowy et al., 2010; Torraca & Mostowy, 2016). In NIH 3T3 fibroblasts and murine endothelial cells, CDC42EP1 binds to SEPTINs (Burbelo et al., 1999; Hirsch et al., 2001; Joberty et al., 1999, 2001; Mostowy & Cossart, 2012).

Interestingly, our CDC42 proteomics uncovered SEPTIN-2 and SEPTIN-7 as binding partners (Figure 1a). SEPTIN-2, SEPTIN-7, and SEPTIN-9 are recruited to bacterial invasion sites and have been implicated for efficient *Salmonella* invasion (Boddy et al., 2018). We performed immunostaining for CDC42EP1 and SEPTIN-7 in C2Bbe1 cells infected by *S.* Typhimurium. 10 min after infection, CDC42EP1 and SEPTIN-7 were both enriched at invasion sites, encircling the bacteria (Figure 3f). A similar finding was made for Villin and CDC42EP1 (Figure 3g). These results suggest that an *S.* Typhimurium infection may recruit a CDC42EP1 complex including SEPTIN-7 and Villin to intracellular bacterial sites.

Wild-type *S.* Typhimurium induces phagocytosis in epithelial cells by activating CDC42 via guanine nucleotide exchange factors (GEFs) SopE and SopE2 (Hardt et al., 1998; Stender et al., 2000). The mutant *S.* Typhimurium strain 14028 S lacks SopE with reduced virulence (Clark et al., 2011; Unsworth et al., 2004; Zhang et al., 2002). Infection of C2Bbe1 cells with wild-type *S.* Typhimurium SL1344 and mutant strain 14028 S demonstrated a significantly reduced invasion by the strain 14028 S (Figure 3h). Interestingly, this reduced invasiveness by SopE-deficient bacteria also failed to robustly recruit CDC42EP1 (Figure 3i,j), suggesting that *S.* Typhimurium strains of varying virulence recruit CDC42EP1 to different degrees. Overexpression of either CDC42 variant or CDC42EP1 failed to affect *S.* Typhimurium's capability of invading the cells (Supporting Information: Figure 3c, 3d, 3e), suggesting that simply increasing CDC42 or CDC42EP1 abundances does not promote *S.* Typhimurium's invasive capability. These results suggest that *S.* Typhimurium-mediated CDC42EP1 recruitment might be a part of its engagement with the host CDC42 machinery.

### 2.4 | CDC42 is required for CDC42EP1 recruitment at bacterial invasion sites

Although the requirement of CDC42 for *S.* Typhimurium invasion was shown in nonintestinal epithelial cells (Brown et al., 2007; Chen et al., 1996; Hardt et al., 1998), few studies on the requirement of CDC42 have been carried out in human enterocytes, the primary target cell type of *Salmonella* infection. Some groups have utilized Caco-2 colonic epithelial cells to demonstrate the role of CDC42-interacting proteins, such as N-WASP and GTPase-activating proteins, during *S.* Typhimurium infections (Davidson et al., 2015, 2023; Higashide et al., 2002). Therefore, we focused our infection experiments on Caco-2 and C2Bbe1 human enterocytes. Infections in both cell lines led to largely similar results in terms of CDC42EP1 redistribution. A head-to-head comparison of these two cell lines showed that *S.* Typhimurium induced a 1.8-fold higher infection in C2Bbe1 cells than in Caco-2 cells (Supporting Information: Figure 4a), likely due to higher apical Villin expression in C2Bbe1 cells (Lhocine et al., 2015).

We then utilized the lentiviral-mediated knockdown strategy and derived a stable CDC42-KD C2Bbe1 cell line (Figure 4a). Invasion of *S.* Typhimurium was significantly reduced in these CDC42-KD C2Bbe1 cells (Figure 4b,c), supporting that CDC42 is required for *Salmonella* invasion in C2Bbe1 cells. Compared with control C2Bbe1 cells, we detected a reduction of CDC42EP1 recruitment to the actin-associated encirclement around invading bacteria in CDC42-KD C2Bbe1 cells (Figure 4c,d). Close examination of these intracellular bacteria revealed that 75% of invading bacteria in control cells had induced an actin

ruffling, and 80% of these actin-encircled bacteria were also CDC42EP1-positive (Figure 4d). However, in CDC42-KD C2Bbe1 cells, only 22% of invading bacteria were actin-encircled, and only 50% of that population was CDC42EP1-positive (Figure 4d). These results suggest that CDC42 is required for both actin and CDC42EP1 recruitment around invading bacteria. Furthermore, in control C2Bbe1 cells, 2% of invading bacteria were encircled by CDC42EP1 without actin, while 33% of invading bacteria in CDC42-KD cells were encircled by CDC42EP1 without actin (Figure 4d), suggesting that CDC42-KD cells were less efficient at reorganizing actin around invading bacteria. Over the course of 30 min, the amount of CDC42EP1-encircled bacteria stayed relatively constant and significantly lower than the number observed in wild-type (WT) cells (Figure 3e), further confirming the deficiency in CDC42EP1 recruitment in the absence of CDC42. Using a previously reported stable CDC42 knockdown Caco-2 cell line (Sakamori et al., 2012), we also observed a reduction in bacterial invasion at 30-min postinfection (Supporting Information: Figure 4b). These data demonstrate that CDC42 deficiency reduces *S.* Typhimurium invasion and impacts CDC42EP1 recruitment around invading bacteria.

### 2.5 | CDC42EP1 deficiency affects intracellular replication or survival, but not initial invasion, of S. typhimurium

To examine the function of CDC42EP1 in *S.* Typhimurium infection, we used lentiviral-small hairpin RNAs (shRNA) particles against CDC42EP1 and established CDC42EP1-KD C2Bbe1 cells (Figure 5a). We performed infection experiments and observed that infected CDC42EP1-KD cells, due to a partial knockdown, exhibited reduced CDC42EP1 around actin-positive intracellular bacteria after 5 min of infection (Figure 5b,c). Since actin-ruffling was still observed around numerous bacteria, indicating successful entry into the cells, the data suggested that CDC42EP1 may not be required to encircle the bacteria for successful invasion. To confirm this, we performed an invasion assay using the CDC42EP1-KD cells and found that the absence of CDC42EP1 did not significantly reduce or enhance the amount of *S.* Typhimurium capable of infecting the cells after 30 min (Figure 5d).

Upon invasion, *S.* Typhimurium utilizes SPI-2 to form a protective niche in the host cell (Hansen-Wester & Hensel, 2001). Since CDC42EP1 was found to associate with intracellular bacteria after a 5-h infection (Figure 2i), we hypothesized that it may play a significant role in events downstream of the initial invasion, such as intracellular replication or survival. We, therefore, performed a longer infection assay to determine how intracellular bacteria survive over time. WT, CDC42-KD, and CDC42EP1-KD C2Bbe1 cells were infected for 30 min, followed by a gentamicin wash-out of extracellular bacteria, and were continuously cultured for 4.5 h before analysis. We found that CDC42-KD and CDC42EP1-KD cells had significantly reduced fold-changes in intracellular bacterial abundance after 5 h, relative to the colony-forming units (CFU) at 30 min (Figure 5e), suggesting that the absence of either CDC42 or CDC42EP1 impairs the intracellular bacteria's growth or survivability. Together, these results demonstrate that expression of CDC42EP1 does not significantly impact initial invasion, but its association with (Figure 2i) and impact on bacterial growth (Figure 5e) after a 5-h infection suggest the absence of CDC42EP1 impairs *S.* Typhimurium survival in IECs.

## 3 | DISCUSSION

A major goal of this study was to clarify the function of CDC42EP1, particularly how it functions in concert with CDC42 during pathogen infections in IECs. Previously, the function of CDC42EP1 has been poorly described, and it is most well-known as a binding partner of Rho GTPase CDC42 and septins (Farrugia & Calvo, 2016; Hirsch et al., 2001; Joberty et al., 2001). Our present study confirmed the interaction of CDC42EP1 with CDC42, but our results go beyond previous reports to show that this interaction is enhanced when CDC42 is in its active conformation and possesses its prenylation modification. Since active, GTP-bound CDC42 is enriched at the plasma membrane (Hoffman et al., 2000; Johnson, 1999; Wedlich-Soldner et al., 2003), CDC42EP1 potentially serves its function at the cell periphery.

*S*. Typhimurium recruit and exploit several host cytoskeletal proteins upon initial invasion into host IECs. We have shown here that CDC42EP1's localization is altered upon infection as it assembles around invading bacteria. Our data suggest that CDC42EP1 recruitment to invading *S*. Typhimurium is dependent on CDC42 activation, as seen by the absence of CDC42EP1 around invading SopE—*S*. Typhimurium and around WT *S*. Typhimurium in CDC42-KD cells. Interestingly, our data demonstrates that, unlike CDC42, CDC42EP1 is not required for successful bacterial internalization. After a 30-min infection in CDC42EP1-KD cells, our invasion assays demonstrate the bacteria are capable of invading as successfully as in WT IECs, and the enrichment of actin ruffles around the bacteria indicate that *S*. Typhimurium are capable of activating CDC42, even in the absence of CDC42EP1. Additionally, unlike septins, which can both aid and inhibit bacterial infections, CDC42EP1 solely plays a role in facilitating *Salmonella* infections, as its absence fails to promote bacterial invasion and survival. Together these data describe a novel pathogenic process: *S*. Typhimurium activate CDC42 which then recruits CDC42EP1 to the bacteria. The slight presence of CDC42EP1 around invading bacteria in the CDC42-KD cells can be attributed to the residual CDC42 expression, and the reduction in actin around CDC42EP1-positive bacteria in these cells may be due to the absence of CDC42, as it is responsible for remodeling actin.

Although depletion of CDC42EP1 does not impact *S*. Typhimurium initial invasion into IECs, we showed that a reduction of both CDC42 and CDC42EP1 impair bacterial survival within host cells 5 h after infection. CDC42 has pleiotropic functions in polarized epithelial cells (Etienne-Manneville, 2004; Harris & Tepass, 2010), and is necessary for cellular proliferation, differentiation, and migration in mouse intestinal epithelia (Melendez et al., 2013; Sakamori et al., 2012). Therefore, the decrease in bacterial survival or replication in CDC42-KD cells may be attributed to disruptions in vesicular trafficking or cellular polarity due to the loss of CDC42. Loss of CDC42EP1 also impaired bacterial survival after a longer infection, but as a downstream effector of CDC42, it may elicit more specific cellular effects and would be a better protein target for preventing successful *S*. Typhimurium colonization. Further evaluation of the role of CDC42EP1 in bacterial intracellular survival can utilize SPI-2 deficient *S*. Typhimurium strains to observe if CDC42EP1 continues to impact bacterial growth. Additionally, since we have shown CDC42EP1 transcript and protein levels increased upon SFB colonization, and it also assembles around invading *S*.

Typhimurium in IECs, CDC42EP1 may regulate the entry and survival of other enteric pathogens.

However, further research is required to fully clarify the function of CDC42EP1, particularly during *S.* Typhimurium infection. Although CDC42EP1 localizes to sites of bacterial entry, its presence does not irrefutably establish any significance or function during invasion. Additionally, other CDC42EP's (CDC42EP2–5) may serve redundant functions and assist in bacterial invasion in the absence of CDC42EP1, requiring further investigation into the function of the entire CDC42EP1 family during pathogenic infection. Furthermore, if CDC42EP1 specifically regulates the intracellular survival of *Salmonella*, the specific population of bacteria that CDC42EP1 impacts should be determined, as *Salmonella* can reside and replicate in both the cytosol and within SCVs, and cytosolic and vacuolar *Salmonella* have distinct pathogenic effects (Castanheira & García-Del Portillo, 2017; Knodler, 2015). The bacteria themselves have the capacity to regulate their SCV and induce rupturing to be released into the cytosol for further replication (Luk et al., 2022; Stévenin et al., 2019), and even express different virulence genes when they are cytosolic as opposed to vacuolar (Powers et al., 2021). Cytosolic *Salmonella* also replicate more quickly and account for the majority of replication in other epithelial cell lines (Malik-Kale et al., 2012), so it is possible that CDC42EP1 impacts multiple intracellular populations of the bacteria. Future research can strategically examine which populations are potentially regulated by CDC42EP1 on both a microscopic and genetic level.

Nevertheless, our results cast a new light on the spatial and temporal relationship between CDC42 and CDC42EP1 in *Salmonella* infection of epithelial cells. Our studies show that each protein has a distinct function during *S.* Typhimurium invasion: while CDC42 is necessary for entry in IECs and is activated by extracellular bacteria, CDC42EP1 helps promote bacterial growth and survival after *S.* Typhimurium have been internalized, and it accumulates around intracellular bacteria. It is currently unknown how CDC42EP1 regulates later pathogenic events. With no known enzymatic domains, and domains at which it binds to CDC42 and certain septins (Farrugia & Calvo, 2016; Hirsch et al., 2001; Joberty et al., 1999), CDC42EP1 may potentially function as a scaffolding protein. We speculate that CDC42EP1 may be recruited to the bacteria to form a scaffold for the acquisition of early endosomal or lysosomal markers that assist in forming SCVs. Further research may reveal CDC42EP1 as a regulator of intracellular bacterial growth and a potential therapeutic target for the treatment of pathogen-induced gastroenteritis.

## 4 | METHODS

### 4.1 | Culture of human cell lines

HeLa (ATCC: CCL2) cells and HEK293T (ATCC: CRL-3216) were grown and cultured in Dulbecco's Modified Eagle Medium (DMEM), supplemented with 10% fetal bovine serum (FBS) (Sigma) and 1% penicillin-streptomycin. Caco-2 (ATCC: HTB-37) and C2Bbe1 (ATCC: CRL-2102) cells were grown and cultured in DMEM, supplemented with 20% FBS and 1% penicillin-streptomycin. All cells were kept at 37°C with 5% $CO_2$.

### 4.2 | Bacterial strains and culture conditions

*S.* Typhimurium strain SL1344 was a kind gift from Dr. Beth McCormick (UMass Chan Medical School). *S.* Typhimurium strain was cultured in Luria Broth supplemented with ampicillin at a concentration of 50 μg/mL shaking O/N at 37°C. Bacteria was reinoculated at a dilution of 1:1000 in ampicillin-Luria Broth and shaken for 6 h at 37°C. Bacterial concentration was quantified by determining optical density at 600 nm, and measurements were obtained every hour to determine when the bacteria entered the stationary phase for optimal SPI-1 expression (Bustamante et al., 2008). Bacteria was then pelleted at 3000*g* for 5 min. Bacteria was resuspended in DMEM supplemented with 20% FBS to treat cells at a multiplicity of infection (MOI) of 100, or $10^8$ CFU were resuspended in 200 μL phosphate-buffered saline (PBS) for in vivo mouse infections.

### 4.3 | Plasmid transfection

HeLa cells were grown to 70%–90% confluence before transfection. A total of 2.5 μg of plasmid DNA per 6 cm dish were transfected using Lipofectamine™ 3000 (Thermofisher, L3000008). Twenty-four hours after transfection, cell lysates were collected for further analyses. CDC42-V1 and CDC42-V2 plasmids were constructed using a pQCXIP vector, with human CDC42 transcript 202(CDC42-V1, Ensemble, ENST00000344548.7), or CDC42 transcript 201(CDC42-V2, Ensemble, ENST00000315554.12) inserted after the 3xFLAG tag. pQCXIP-3xFLAG-CDC42-V1-F28L, pQCXIP-3xFLAG-CDC42-V2-C188A, pQCXIP-3xFLAG-CDC42-V2-C189A, and pQCXIP-3xFLAG-CDC42-V2-C188/189A were all generated through site-directed mutageneses using the QuikChange II Site-Directed Mutagenesis Kit (Agilent, Cat#200523). pQCXIP-3xFLAG-HA-V2, pQCXIP-3xFLAG-HA-V2-G12V, and pQCXIP-3xFLAG-HA-V2-T17N were generated by placing the HA-V2 sequences from the following plasmids into the pQCXIP-3xFLAG backbone: CDC42 placental isoform (#CDC42P0000; cDNA Resource Center), CDC42 placental isoform G12V (#CDC42P00C0; cDNA Resource Center), and CDC42 placental isoform T17N (#CDC42P00D0; cDNA Resource Center). pcDNA 3.2/V5-DEST CDC42EP1 WT #69819 was obtained from Addgene.

### 4.4 | Flag-IP and proteomic analysis with mass-spectrometry

HEK293T cells were transfected with either empty pQCXIP-3XFlag Vector, pQCXIP-3XFlag-CDC42V1WT or pQCXIP-3XFlag-CDC42V2WT. Cell lysates were subjected to Flag Immunoprecipitation Kit (Sigma-Aldrich, FLAGIPT1). Pull-down elute was subjected to western blot using NuPAGE™ 4%–12% Bis-Tris Protein Gels (NP0335, ThermoScientific), which was then fixed for 1 h with fixative containing 50% methanol and 10% acetic acid. After staining with Ruby Red, protein bands on the gel were cut out for mass spectrometry analysis at Center for Advanced Proteomics Research of New Jersey Medical School Cancer Research Center. Data were analyzed DAVID Bioinformatics Resources 6.8 and Search Tool for the Retrieval of Interacting Genes/Proteins (STRING, v11.5). Gene Ontology Biological Processes were chosen based on the lowest false discovery rate values.

### 4.5 | Western blot analysis

Cells were lysed with a 0.5% NP-40 nondenaturing lysis buffer followed by disruption using a 20 G needle. Protein concentrations of the lysate were determined using Bradford Assay. A total of ~20 μg of total protein were loaded on 10% sodium dodecyl sulfate-polyacrylamide (SDS-PAGE) gels and run at room temperature. Transfer of proteins from gels onto the nitrocellulose membranes was carried out in a chilled transfer buffer with methanol set at a constant current of 300 mA for 90 min. Membranes were blocked with 5% milk in tris-buffered saline (TBS) with 0.1%Tween-20 (TBS-T) for 1 h at room temperature followed by overnight incubation at 4°C with primary antibodies. The primary antibodies used were as follows: anti-FLAG® (1:10,000, Sigma, F1804), anti-CDC42EP1 (1:1000, Thermofisher, PA5–30433), anti-CDC42 (1:500, Cell Signaling Technologies, 2462 S), and anti-GAPDH (1:2000, Cell Signaling Technologies, 14C10). Membranes were then washed three times in TBS-T and incubated with either anti-mouse (1:2000, GE Healthcare, NA931) or anti-rabbit (1:2000, GE Healthcare, NA934) horseradish peroxidase (HRP)-conjugated secondary antibody for 1 h. They were further washed and developed using enhanced chemiluminescence (ECL) (standard GE healthcare, RPN2209) or ECL prime (GE Healthcare, RPN2232) detection solution in the dark on chemiluminescent sensitive X-Ray film, or using the ChemiDoc™MP Imaging System (BioRad).

### 4.6 | Immunofluorescent staining

Before staining, HeLa cells were grown to confluency, and Caco-2 and C2BBe1 cells were grown to differentiated monolayers and maintained for 2 weeks in four-well chamber slides. After infection with SL1344 at MOI of 100 for varying time points, cells were washed with 150 μg/mL gentamicin to remove extracellular bacteria, fixed with 4% paraformaldehyde (PFA) for 10 min and washed with cold PBS. Cells were then permeabilized with 0.2% Triton X-100 in 5% bovine serum albumin (BSA)-PBS for another 15 min followed by blocking for 1 h in 5%BSA-PBS. Cells were then incubated in primary antibodies at 4°C O/N. The following primary antibodies were used: anti-FLAG® (1:10,000, Sigma, F1804), anti-CDC42EP1 (1:400, Thermofisher, PA5–30433), anti-*Salmonella* (1:1000, Thermofisher, MA1–16686), anti-*Salmonella* (1:1000, Thermofisher, PA1–7244), anti-*Salmonella* (1:1000, BacTrace, 5320–0044), anti-Septin-7 (1:200, Proteintech, 66542–1), anti-Villin (1:200, Santa Cruz, sc-7672) and anti-LAMP1 (1:100; DSHB; H4A3). Cells were washed and incubated with fluorescence-conjugated secondary antibodies and DAPI and Phalloidin-AlexaFlour 647 (1:400, ThermoFisher, A22287) for 1 h at room temperature. Cells were then washed with PBS, allowed to dry, and mounted using Prolong Gold Antifade medium. Images were taken using an LSM 510, 880, or 980 Laser Scanning microscope, and analyzed using ImageJ. Quantification of CDC42EP1+ and Actin+ bacteria was performed by counting all bacteria in ≥ three representative fields.

### 4.7 | In vitro infections

C2Bbe1 and Caco-2 cells were seeded at $10^6$ cells/well in six-well plates (35 mm). Prior experiments measured the transepithelial electric resistance (TEER) of C2Bbe1 cells grown on transwell inserts and demonstrated the cells reach maximal polarization 21 days postconfluency. Therefore, cells were grown to differentiated monolayers and then

maintained for 3 weeks to ensure polarization. Cell culture media was replaced with 20% FBS in DMEM (without penicillin-streptomycin). SL1344 was added to cells at a MOI of 100 and incubated with cells for various timepoints (up to 30 min) at 37°C, 5% $CO_2$. Cells were then washed with 150 μg/mL gentamicin (Corning, #30–005-CR) and lysed for protein/RNA analysis or fixed with 4% PFA for immunocytochemistry. For gentamicin protection assays, cells were incubated with 150 μg/mL gentamicin for 50 min after removal of bacteria, washed once with PBS, lysed with 0.5% Triton X-100 in PBS, and serial dilutions of lysates were plated on xylose lysine deoxycholate (XLD) agar plates for quantifying bacterial growth.

For 5-h gentamicin protection assay, two sets of WT, CDC42-KD, and CDC42EP-1 KD were infected with *S.* Typhimurium at an MOI of 100. Following 30 min of infection, a gentamicin protection assay, as described above, was performed on the first set of cells. After the 30 min infection, the other set of cells was incubated with 150 μg/mL gentamicin for 50 min to remove extracellular bacteria and then replaced with 20% FBS-DMEM to allow any internalized bacteria to grow and survive. Fivehours after the initial infection, the second set of cells were then washed with PBS, lysed with 0.5% Triton X-100 in PBS, and serial dilutions of lysates were plated on XLD agar plates. *S.* Typhimurium CFU were counted from the 30 min infection and from the 5 h infection, and fold changes were calculated to quantify bacterial survival and growth.

### 4.8 | Lentivirus-mediated CDC42 and CDC42EP1 knockdown

To stably knockdown *CDC42* and *CDC42EP1* in C2BBe1 cells, human *CDC42*-specific (#TRCN0000047628; Sigma-Aldrich) and *CDC42EP1*-specific (#TRCN0000296684; Sigma-Aldrich) lentiviral transduction particles were added to cells in serum-free and antibiotic-free media at 1/5 multiplicity of infection. After 6 h, serum and gentamicin were added to the media at concentrations of 20% and 100 μg/mL, respectively. Positively infected cells were screened with media containing 14 μg/mL puromycin 72 h postinfection for 10 additional days. Knockdown cell cultures were maintained in 14 μg/mL puromycin.

### 4.9 | quantitative polymerase chain reaction (qPCR)

RNA was isolated from cells and tissues using the RNeasy Mini Kit (Qiagen, Catalog No. 74104), according to the manufacturer's protocol. RNA was then reverse-transcribed to generate complementary DNA (cDNA) using 1 μg of RNA and the Maxima First Strand cDNA Synthesis Kit for RT-qPCR (ThermoFisher, Catalog No. K1641). SYBR Green Real-Time PCR Master Mixes (Thermo Fisher) were used for all qPCR reactions. The PCR cycling conditions were as follows: 10 min preheating at 95°C followed by 45 cycles of denaturing (95°C for 10 s), annealing (60°C for 10 s), and extension (72°C for 10 s). Hypoxanthine guanine phosphoribosyltransferase was analyzed as a house-keeping gene as an internal reference. The primers used were as follows: CDC42EP1 Forward: 5′TGT GTG AGG CGG ACA GTG G 3′; CDC42EP1 Reverse: 5′AAT CAA GGG TCC TGG CTG CC 3′; CDC42 Forward: 5′ TGACAGATTACGACCGCTGAGTT 3′; CDC42 Reverse: 5′ GGAGTCTTTGGACAGTGGTGAG 3′.

### 4.10 | Quantification and statistical analyses

Mass spectrometry peptide hits from CDC42-V1 and CDC42-V2 pull-down complexes were analyzed using String V11.5 (https://string-db.org/) and DAVID 6.8 (NIH, https://david.ncifcrf.gov/). All immunofluorescent images and western blot images were analyzed using ImageJ (NIH, https://imagej.nih.gov/ij/download.html). Pearson's Correlation using ImageJ; Coloc 2 function was used to analyze regions of interest drawn around invading bacteria. The Costes' randomization was then set to 50, and Pearson's R-value (no Threshold) was recorded. Statistically significant differences were analyzed using a two-tailed Student's *t* test, or one-way analysis of variance (ANOVA) for multigroup comparisons, on Graphpad Prism 9. All micrographs and quantifications are representative of ≥ three independent experiments.

## Supplementary Material

Refer to Web version on PubMed Central for supplementary material.

## Funding information

National Institutes of Health

## REFERENCES

Beuzon CR (2000). Salmonella maintains the integrity of its intracellular vacuole through the action of SifA. The EMBO Journal, 19, 3235–3249. [PubMed: 10880437]

Boddy KC, Gao AD, Truong D, Kim MS, Froese CD, Trimble WS, & Brumell JH (2018). Septin-regulated actin dynamics promote Salmonella invasion of host cells. Cellular Microbiology, 20, e12866. [PubMed: 29885024]

Boyle EC, Brown NF, & Finlay BB (2006). Salmonella enterica serovar typhimurium effectors SopB, SopE, SopE2 and SipA disrupt tight junction structure and function. Cellular Microbiology, 8, 1946–1957. [PubMed: 16869830]

Brown MD, Bry L, Li Z, & Sacks DB (2007). IQGAP1 regulates salmonella invasion through interactions with actin, Rac1, and Cdc42. Journal of Biological Chemistry, 282, 30265–30272. [PubMed: 17693642]

Burbelo PD, Snow DM, Bahou W, & Spiegel S (1999). MSE55, a Cdc42 effector protein, induces long cellular extensions in fibroblasts. Proceedings of the National Academy of Sciences, 96, 9083–9088.

Bustamante VH, Martínez LC, Santana FJ, Knodler LA, Steele-Mortimer O, & Puente JL (2008). HilD-mediated transcriptional cross-talk between SPI-1 and SPI-2. Proceedings of the National Academy of Sciences, 105, 14591–14596.

Castanheira S, & García-Del Portillo F (2017). Salmonella populations inside host cells. Frontiers in Cellular and Infection Microbiology, 7, 432. [PubMed: 29046870]

Chen L-M, Hobbie S, & Galán JE (1996). Requirement of CDC42 for Salmonella-Induced cytoskeletal and nuclear responses. Science (New York, N.Y.), 274, 2115–2118. [PubMed: 8953049]

Clark L, Perrett CA, Malt L, Harward C, Humphrey S, Jepson KA, Martinez-Argudo I, Carney LJ, La Ragione RM, Humphrey TJ, & Jepson MA (2011). Differences in salmonella enterica serovar typhimurium strain invasiveness are associated with heterogeneity in SPI-1 gene expression. Microbiology, 157, 2072–2083. [PubMed: 21493681]

Cooper JA (1987). Effects of cytochalasin and phalloidin on actin. The Journal of Cell Biology, 105, 1473–1478. [PubMed: 3312229]

Davidson A, Hume PJ, Greene NP, & Koronakis V (2023). Salmonella invasion of a cell is self-limiting due to effector-driven activation of N-WASP. iScience, 26, 106643. [PubMed: 37168569]

Davidson AC, Humphreys D, Brooks ABE, Hume PJ, & Koronakis V (2015). The arf GTPase-activating protein family is exploited by salmonella enterica serovar typhimurium to invade nonphagocytic host cells. mBio, 6(1), e02253–14. [PubMed: 25670778]

Eng S-K, Pusparajah P, Ab Mutalib N-S, Ser H-L, Chan K-G, & Lee L-H (2015). Salmonella: A review on pathogenesis, epidemiology and antibiotic resistance. Frontiers in Life Science, 8, 284–293.

Etienne-Manneville S (2004). Cdc42--the centre of polarity. Journal of Cell Science, 117, 1291–1300. [PubMed: 15020669]

Farrugia AJ, & Calvo F (2016). The borg family of Cdc42 effector proteins Cdc42EP1–5. Biochemical Society Transactions, 44, 1709–1716. [PubMed: 27913681]

Figueira R, & Holden DW (2012). Functions of the salmonella pathogenicity island 2 (SPI-2) type III secretion system effectors. Microbiology, 158, 1147–1161. [PubMed: 22422755]

Finlay BB, & Falkow S (1990). Salmonella interactions with polarized human intestinal Caco-2 epithelial cells. Journal of Infectious Diseases, 162, 1096–1106. [PubMed: 2230236]

Finlay BB, Ruschkowski S, & Dedhar S (1991). Cytoskeletal rearrangements accompanying salmonella entry into epithelial cells. Journal of Cell Science, 99(Pt 2), 283–296. [PubMed: 1909337]

Francis CL, Ryan TA, Jones BD, Smith SJ, & Falkow S (1993). Ruffles induced by salmonella and other stimuli direct macropinocytosis of bacteria. Nature, 364, 639–642. [PubMed: 8350922]

Fu Y, & Galán JE (1999). A salmonella protein antagonizes Rac-1 and Cdc42 to mediate host-cell recovery after bacterial invasion. Nature, 401, 293–297. [PubMed: 10499590]

Galán JE (2001). Salmonella interactions with host cells: type III secretion at work. Annual Review of Cell and Developmental Biology, 17, 53–86.

Gomes AQ, Ali BR, Ramalho JS, Godfrey RF, Barral DC, Hume AN, & Seabra MC (2003). Membrane targeting of rab GTPases is influenced by the prenylation motif. Molecular Biology of the Cell, 14, 1882–1899. [PubMed: 12802062]

Hansen-Wester I, & Hensel M (2001). Salmonella pathogenicity islands encoding type III secretion systems. Microbes and Infection, 3, 549–559. [PubMed: 11418329]

Hardt WD, Chen LM, Schuebel KE, Bustelo XR, & Galán JE (1998). S. typhimurium encodes an activator of Rho GTPases that induces membrane ruffling and nuclear responses in host cells. Cell, 93, 815–826. [PubMed: 9630225]

Harris KP, & Tepass U (2010). Cdc42 and vesicle trafficking in polarized cells. Traffic, 11, 1272–1279. [PubMed: 20633244]

Haspel N, Jang H, & Nussinov R (2021). Active and inactive Cdc42 differ in their insert region conformational dynamics. Biophysical Journal, 120, 306–318. [PubMed: 33347888]

Hayward RD (1999). Direct nucleation and bundling of actin by the SipC protein of invasive salmonella. The EMBO Journal, 18, 4926–4934. [PubMed: 10487745]

Hayward RD, & Koronakiss V (2002). Direct modulation of the host cell cytoskeleton by salmonella actin-binding proteins. Trends in Cell Biology, 12, 15–20. [PubMed: 11854005]

Higashide W, Dai S, Hombs VP, & Zhou D (2002). Involvement of SipA in modulating actin dynamics during salmonella invasion into cultured epithelial cells. Cellular Microbiology, 4, 357–365. [PubMed: 12116966]

Hirsch DS, Pirone DM, & Burbelo PD (2001). A new family of Cdc42 effector proteins, CEPs, function in fibroblast and epithelial cell shape changes. Journal of Biological Chemistry, 276, 875–883. [PubMed: 11035016]

Hoffman GR, Nassar N, & Cerione RA (2000). Structure of the Rho family GTP-binding protein Cdc42 in complex with the multifunctional regulator RhoGDI. Cell, 100, 345–356. [PubMed: 10676816]

Joberty G, Perlungher RR, & Macara IG (1999). The borgs, a new family of Cdc42 and TC10 GTPase-interacting proteins. Molecular and Cellular Biology, 19, 6585–6597. [PubMed: 10490598]

Joberty G, Perlungher RR, Sheffield PJ, Kinoshita M, Noda M, Haystead T, & Macara IG (2001). Borg proteins control septin organization and are negatively regulated by Cdc42. Nature Cell Biology, 3, 861–866. [PubMed: 11584266]

Johnson DI (1999). Cdc42: an essential rho-type GTPase controlling eukaryotic cell polarity. Microbiology and Molecular Biology Reviews, 63, 54–105. [PubMed: 10066831]

Kang R, Wan J, Arstikaitis P, Takahashi H, Huang K, Bailey AO, Thompson JX, Roth AF, Drisdel RC, Mastro R, Green WN, Yates III JR, Davis NG, & El-Husseini A (2008). Neural palmitoyl-proteomics reveals dynamic synaptic palmitoylation. Nature, 456, 904–909. [PubMed: 19092927]

Knodler LA (2015). Salmonella enterica: living a double life in epithelial cells. Current Opinion in Microbiology, 23, 23–31. [PubMed: 25461569]

Kubori T, & Galán JE (2003). Temporal regulation of salmonella virulence effector function by proteasome-dependent protein degradation. Cell, 115, 333–342. [PubMed: 14636560]

Kubori T, Sukhan A, Aizawa SI, & Galán JE (2000). Molecular characterization and assembly of the needle complex of the salmonella typhimurium type III protein secretion system. Proceedings of the National Academy of Sciences, 97, 10225–10230.

Ladinsky MS, Araujo LP, Zhang X, Veltri J, Galan-Diez M, Soualhi S, Lee C, Irie K, Pinker EY, Narushima S, Bandyopadhyay S, Nagayama M, Elhenawy W, Coombes BK, Ferraris RP, Honda K, Iliev ID, Gao N, Bjorkman PJ, & Ivanov II (2019). Endocytosis of commensal antigens by intestinal epithelial cells regulates mucosal T cell homeostasis. Science, 363, eaat4042. [PubMed: 30846568]

Leung DW, & Rosen MK (2005). The nucleotide switch in Cdc42 modulates coupling between the GTPase-binding and allosteric equilibria of Wiskott-Aldrich syndrome protein. Proceedings of the National Academy of Sciences of the United States of America, 102, 5685–5690. [PubMed: 15821030]

Lhocine N, Arena ET, Bomme P, Ubelmann F, Prévost MC, Robine S, & Sansonetti PJ (2015). Apical invasion of intestinal epithelial cells by salmonella typhimurium requires villin to remodel the brush border actin cytoskeleton. Cell Host & Microbe, 17, 164–177. [PubMed: 25600187]

Lin Q, Fuji RN, Yang W, & Cerione RA (2003). RhoGDI is required for Cdc42-mediated cellular transformation. Current Biology, 13, 1469–1479. [PubMed: 12956948]

Liu Z, Vong QP, Liu C, & Zheng Y (2014). Borg5 is required for angiogenesis by regulating persistent directional migration of the cardiac microvascular endothelial cells. Molecular Biology of the Cell, 25, 841–851. [PubMed: 24451259]

Luk CH, Enninga J, & Valenzuela C (2022). Fit to dwell in many places—the growing diversity of intracellular salmonella niches. Frontiers in Cellular and Infection Microbiology, 12, 989451. [PubMed: 36061869]

Malik-Kale P, Winfree S, & Steele-Mortimer O (2012). The bimodal lifestyle of intracellular salmonella in epithelial cells: Replication in the cytosol obscures defects in vacuolar replication. PLoS ONE, 7, e38732. [PubMed: 22719929]

Marks PW, & Kwiatkowski DJ (1996). Genomic organization and chromosomal location of murine Cdc42. Genomics, 38, 13–18. [PubMed: 8954774]

Martin LJ, Fyfe M, Doré K, Buxton JA, Pollari F, Henry B, Middleton D, Ahmed R, Jamieson F, Ciebin B, McEwen SA, & Wilson JB (2004). Increased burden of illness associated with antimicrobial-resistant salmonella enterica serotype typhimurium infections. The Journal of infectious diseases, 189, 377–384. [PubMed: 14745694]

Melendez J, Liu M, Sampson L, Akunuru S, Han X, Vallance J, Witte D, Shroyer N, & Zheng Y (2013). Cdc42 coordinates proliferation, polarity, migration, and differentiation of small intestinal epithelial cells in mice. Gastroenterology, 145, 808–819. [PubMed: 23792201]

Moon SS, Rahman AA, Kim JY, & Kee SH (2008). Hanultarin, a cytotoxic lignan as an inhibitor of actin cytoskeleton polymerization from the seeds of trichosanthes kirilowii. Bioorganic & Medicinal Chemistry, 16, 7264–7269. [PubMed: 18603435]

Mostowy S, Bonazzi M, Hamon MA, Tham TN, Mallet A, Lelek M, Gouin E, Demangel C, Brosch R, Zimmer C, Sartori A, Kinoshita M, Lecuit M, & Cossart P (2010). Entrapment of intracytosolic bacteria by septin cage-like structures. Cell Host & Microbe, 8, 433–444. [PubMed: 21075354]

Mostowy S, & Cossart P (2012). Septins: the fourth component of the cytoskeleton. Nature Reviews Molecular Cell Biology, 13, 183–194. [PubMed: 22314400]

Murli S, Watson RO, & Galan JE (2001). Role of tyrosine kinases and the tyrosine phosphatase SptP in the interaction of salmonella with host cells. Cellular Microbiology, 3, 795–810. [PubMed: 11736992]

Nishimura A, & Linder ME (2013). Identification of a novel prenyl and palmitoyl modification at the CaaX motif of Cdc42 that regulates RhoGDI binding. Molecular and Cellular Biology, 33, 1417–1429. [PubMed: 23358418]

Nobes CD, & Hall A (1995). Rho, rac and cdc42 GTPases: regulators of actin structures, cell adhesion and motility. Biochemical Society Transactions, 23, 456–459. [PubMed: 8566347]

Patel JC, & Galán JE (2005). Manipulation of the host actin cytoskeleton by salmonella—all in the name of entry. Current Opinion in Microbiology, 8, 10–15. [PubMed: 15694851]

Peterson MD, & Mooseker MS (1992). Characterization of the enterocyte-like brush border cytoskeleton of the C2BBe clones of the human intestinal cell line, Caco-2. Journal of Cell Science, 102(Pt 3), 581–600. [PubMed: 1506435]

Powers TR, Haeberle AL, Predeus AV, Hammarlöf DL, Cundiff JA, Saldaña-Ahuactzi Z, Hokamp K, Hinton JCD, & Knodler LA (2021). Intracellular niche-specific profiling reveals transcriptional adaptations required for the cytosolic lifestyle of salmonella enterica. PLoS Pathogens, 17, e1009280. [PubMed: 34460873]

Que F, Wu S, & Huang R (2013). Salmonella pathogenicity island 1(SPI-1) at work. Current Microbiology, 66, 582–587. [PubMed: 23370732]

Richter S, Martin R, Gutzeit HO, & Knölker HJ (2021). In vitro and in vivo effects of inhibitors on actin and myosin. Bioorganic & Medicinal Chemistry, 30, 115928. [PubMed: 33341499]

Roberts PJ, Mitin N, Keller PJ, Chenette EJ, Madigan JP, Currin RO, Cox AD, Wilson O, Kirschmeier P, & Der CJ (2008). Rho family GTPase modification and dependence on CAAX motif-signaled posttranslational modification. Journal of Biological Chemistry, 283, 25150–25163. [PubMed: 18614539]

Rodríguez-Escudero I, Ferrer NL, Rotger R, Cid VJ, & Molina M (2011). Interaction of the salmonella typhimurium effector protein SopB with host cell Cdc42 is involved in intracellular replication. Molecular Microbiology, 80, 1220–1240. [PubMed: 21435037]

Sakamori R, Das S, Yu S, Feng S, Stypulkowski E, Guan Y, Douard V, Tang W, Ferraris RP, Harada A, Brakebusch C, Guo W, & Gao N (2012). Cdc42 and Rab8a are critical for intestinal stem cell division, survival, and differentiation in mice. Journal of Clinical Investigation, 122, 1052–1065. [PubMed: 22354172]

Schlumberger MC, Müller AJ, Ehrbar K, Winnen B, Duss I, Stecher B, & Hardt WD (2005). Real-time imaging of type III secretion: Salmonella SipA injection into host cells. Proceedings of the National Academy of Sciences, 102, 12548–12553.

Sinha S, & Yang W (2008). Cellular signaling for activation of rho GTPase Cdc42. Cellular Signalling, 20, 1927–1934. [PubMed: 18558478]

Steele-Mortimer O (2008). The salmonella-containing vacuole: Moving with The Times. Current Opinion in Microbiology, 11, 38–45. [PubMed: 18304858]

Steele-Mortimer O, Meresse S, Gorvel JP, Toh BH, & Finlay BB (1999). Biogenesis of salmonella typhimurium-containing vacuoles in epithelial cells involves interactions with the early endocytic path-way. Cellular Microbiology, 1, 33–49. [PubMed: 11207539]

Stender S, Friebel A, Linder S, Rohde M, Mirold S, & Hardt WD (2000). Identification of SopE2 from salmonella typhimurium, a conserved guanine nucleotide exchange factor for Cdc42 of the host cell. Molecular Microbiology, 36, 1206–1221. [PubMed: 10931274]

Stévenin V, Chang YY, Le Toquin Y, Duchateau M, Gianetto QG, Luk CH, Salles A, Sohst V, Matondo M, Reiling N, & Enninga J (2019). Dynamic growth and shrinkage of the salmonella-containing vacuole determines the intracellular pathogen niche. Cell Reports, 29, 3958–3973. [PubMed: 31851926]

Tafazoli F, Magnusson KE, & Zheng L (2003). Disruption of epithelial barrier integrity by salmonella enterica serovar typhimurium requires geranylgeranylated proteins. Infection and Immunity, 71, 872–881. [PubMed: 12540569]

Torraca V, & Mostowy S (2016). Septins and bacterial infection. Frontiers in Cell and Developmental Biology, 4, 127. [PubMed: 27891501]

Unsworth KE, Way M, McNiven M, Machesky L, & Holden DW (2004). Analysis of the mechanisms of salmonella-induced actin assembly during invasion of host cells and intracellular replication. Cellular Microbiology, 6, 1041–1055. [PubMed: 15469433]

Usui T, Kazami S, Dohmae N, Mashimo Y, Kondo H, Tsuda M, Terasaki AG, Ohashi K, Kobayashi J, & Osada H (2004). Amphidinolide h, a potent cytotoxic macrolide, covalently binds on actin subdomain 4 and stabilizes actin filament. Chemistry & Biology, 11, 1269–1277. [PubMed: 15380187]

Vong QP, Liu Z, Yoo JG, Chen R, Xie W, Sharov AA, Fan CM, Liu C, Ko MSH, & Zheng Y (2010). A role for borg5 during trophectoderm differentiation. Stem Cells, 28, 1030–1038. [PubMed: 20506138]

Wedlich-Soldner R, Altschuler S, Wu L, & Li R (2003). Spontaneous cell polarization through actomyosin-based delivery of the Cdc42 GTPase. Science, 299, 1231–1235. [PubMed: 12560471]

Wirth A, Chen-Wacker C, Wu YW, Gorinski N, Filippov MA, Pandey G, & Ponimaskin E (2013). Dual lipidation of the brain-specific Cdc42 isoform regulates its functional properties. Biochemical Journal, 456, 311–322. [PubMed: 24059268]

Yap K, Xiao Y, Friedman BA, Je HS, & Makeyev EV (2016). Polarizing the neuron through sustained co-expression of alternatively spliced isoforms. Cell Reports, 15, 1316–1328. [PubMed: 27134173]

Zhang S, Santos RL, Tsolis M, Mirold S, Hardt WD, Adams LG, & Bäumler AJ (2002). Phage mediated horizontal transfer of the sopE1 gene increases enteropathogenicity of salmonella enterica serotype typhimurium for calves. FEMS Microbiology Letters, 217, 243–247. [PubMed: 12480111]

Zhang X, Bandyopadhyay S, Araujo LP, Tong K, Flores J, Laubitz D, Zhao Y, Yap G, Wang J, Zou Q, Ferraris R, Zhang L, Hu W, Bonder EM, Kiela PR, Coffey R, Verzi MP, Ivanov II, & Gao N (2020). Elevating EGFR-MAPK program by a nonconventional Cdc42 enhances intestinal epithelial survival and regeneration. JCI Insight, 5(16), e135923. [PubMed: 32686657]

Zhou D, Chen LM, Hernandez L, Shears SB, & Galan JE (2001). A salmonella inositol polyphosphatase acts in conjunction with other bacterial effectors to promote host cell actin cytoskeleton rearrangements and bacterial internalization. Molecular Microbiology, 39, 248–260. [PubMed: 11136447]

Zhou D, Mooseker MS, & Galán JE (1999). Role of the S. typhimurium actin-binding protein SipA in bacterial internalization. Science, 283, 2092–2095. [PubMed: 10092234]

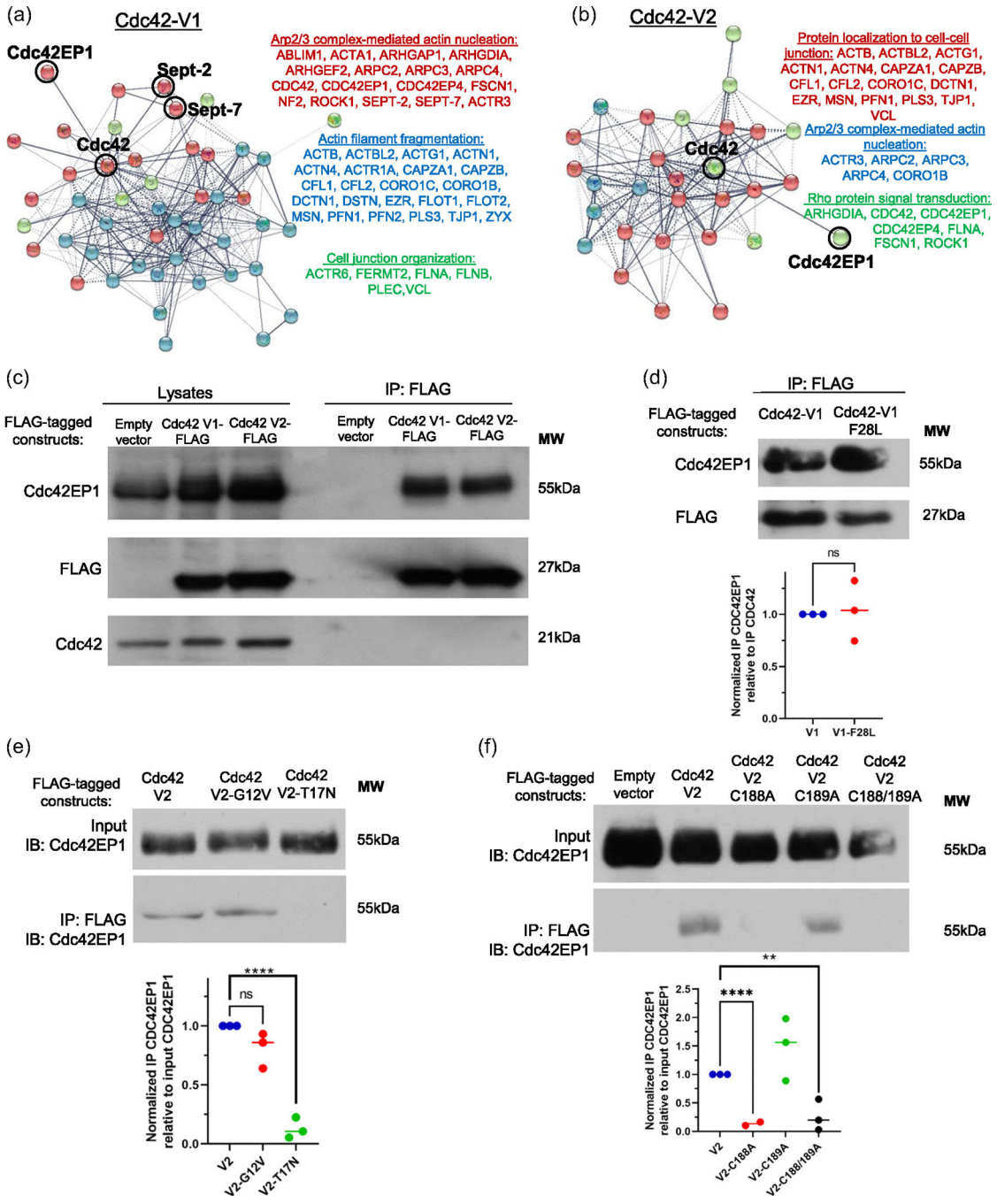


**FIGURE 1.**

CDC42EP1 interacts with CDC42. (a, b) Proteomic analysis by mass spectrometry uncovered interactome of 3xFLAG-tagged-CDC42-V1 or CDC42-V2 in HEK293T cells. Unsupervised clustering using Search Tool for the Retrieval of Interacting Genes/Proteins (STRING v11.5) revealed clusters of proteins involved in the indicated Gene Ontology (GO) Biological Processes. All GO Biological Process terms had a *p*-value < 0.00001. (c) Immunoblot of CDC42EP1, FLAG, and CDC42 after immunoprecipitation using a FLAG antibody in HEK293T cells transfected with 3xFLAG (empty) vector, 3xFLAG-CDC42-V1,

or 3xFLAG-CDC42-V2. Immunoblot is representative of three independent experiments. (d) Immunoblot of CDC42EP1 and FLAG after immunoprecipitation using a FLAG antibody in HEK293T cells transfected with 3xFLAG-CDC42-V1 or 3xFLAG-CDC42-V1-F28L. Immunoblot is representative of three independent experiments. Quantification is provided below. (e) Immunoblot of CDC42EP1 after immunoprecipitation of FLAG in HEK293T cells after transfection with 3xFLAG-HA-CDC42-V2, 3xFLAG-HA-CDC42-V2-G12V, or 3xFLAG-HA-CDC42-V2-T17N. Quantification is provided below. (f) Immunoblot of CDC42EP1 after immunoprecipitation of FLAG in HEK293T cells after transfection with 3xFLAG-HA-CDC42-V2, 3xFLAG-HA-CDC42-V2-C188A, 3xFLAG-HA-CDC42-V2-C189A, or 3xFLAG-HA-CDC42-V2-C188/189A. Quantification provided below.

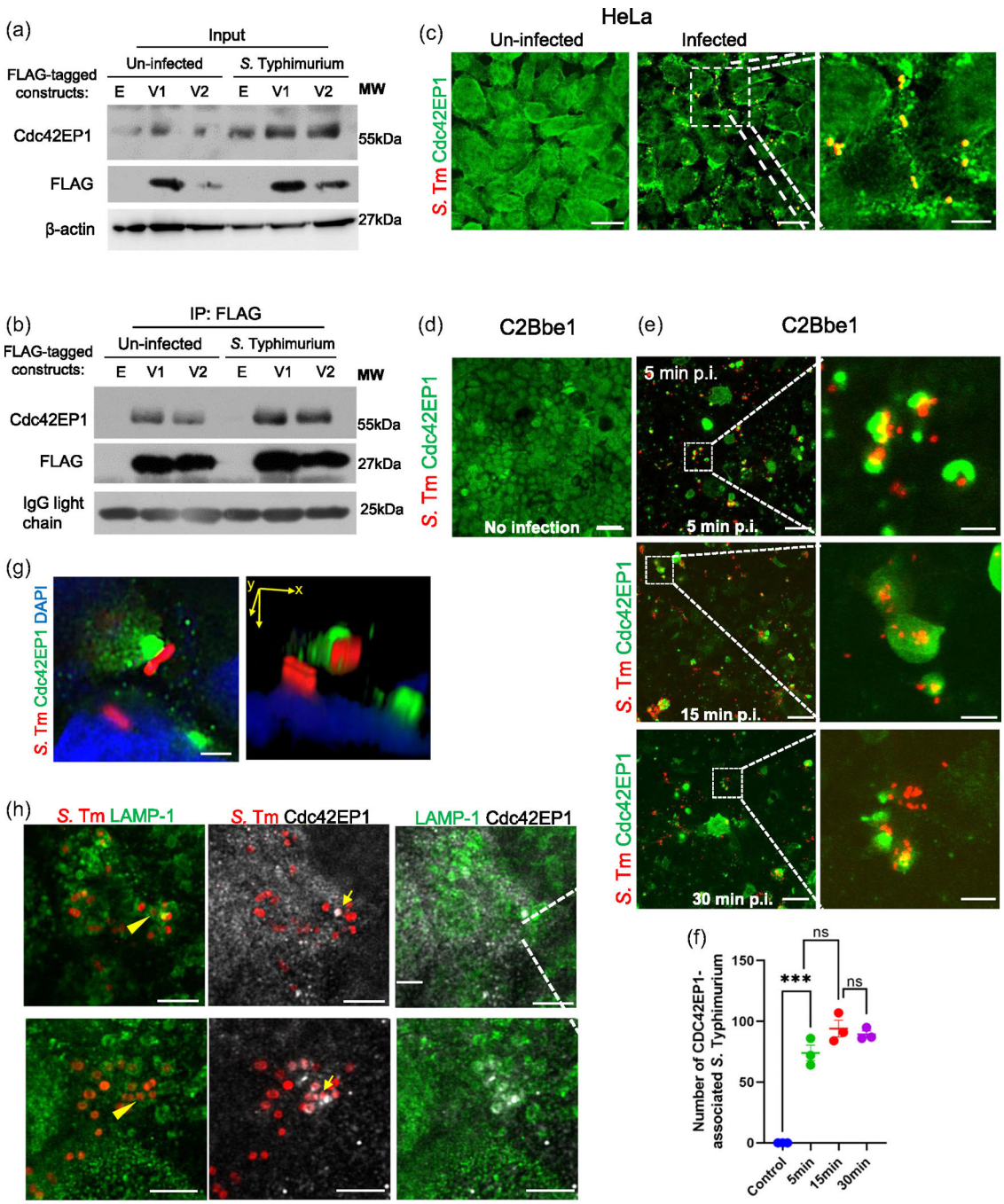


**FIGURE 2.**

*S.* Typhimurium infection rapidly alters CDC42EP1 localization. (a) Immunoblot of CDC42EP1 and FLAG of HEK293T lysates after 30 min of *S.* Typhimurium infection in cells transfected with 3xFLAG vector (E: empty vector), 3xFLAG-CDC42-V1, or 3xFLAG-CDC42-V2 before and after a 30-min *S.* Typhimurium infection. (b) Immunoblot of CDC42EP1 and FLAG after immunoprecipitation using a FLAG antibody from lysates shown in panel a. (c) Immunofluorescent images of *Salmonella* (red) and CDC42EP1 (green) in HeLa cells before (uninfected) and after a 5-min *S.* Typhimurium infection. Scale

bar for low-magnification images represent 25 μm and for high-magnification image is 10 μm. (d,e) Representative immunofluorescent images of *Salmonella* (red) and CDC42EP1 (green) in C2Bbe1 cells before infection (d), and 5-min, 15-min, and 30-min postinfection (p.i.) (e). Scale bar is for the low-magnification image is 50 μm and the scale bar for higher magnification of insets is 10 μm. (f) Quantification of the number of CDC42EP1-associated internalized *S.* Typhimurium after each infection timepoint represented in panels d-f. Bacteria were counted from three independent microscopic fields containing approximately 150 internalized bacteria per image. (g) Immunofluorescent image of CDC42EP1 (green) and *Salmonella* (red) in C2Bbe1 cells 5 min postinfection taken on Zeiss LSM 880 using Airyscan. XY-plane image (top) and 3D-render (bottom) depict small puncta of CDC42EP1 approaching a bacterium. Scale bar represents 2 μm. (h) Representative immunostaining of *Salmonella* (red) and lysosome-associated membrane protein (LAMP)-1 (green) in C2Bbe1 cells 5 h after a 30 min initial infection. Yellow arrows highlight regions of intense CDC42EP1 expression on *Salmonella*-containing vacuoles (SCV)-associated bacteria. Yellow arrowheads highlight LAMP-1 expression encircling bacteria, indicative of SCV formation. All scale bars represent 5 μm. Micrographs acquired on Zeiss LSM 980 using Airyscan.

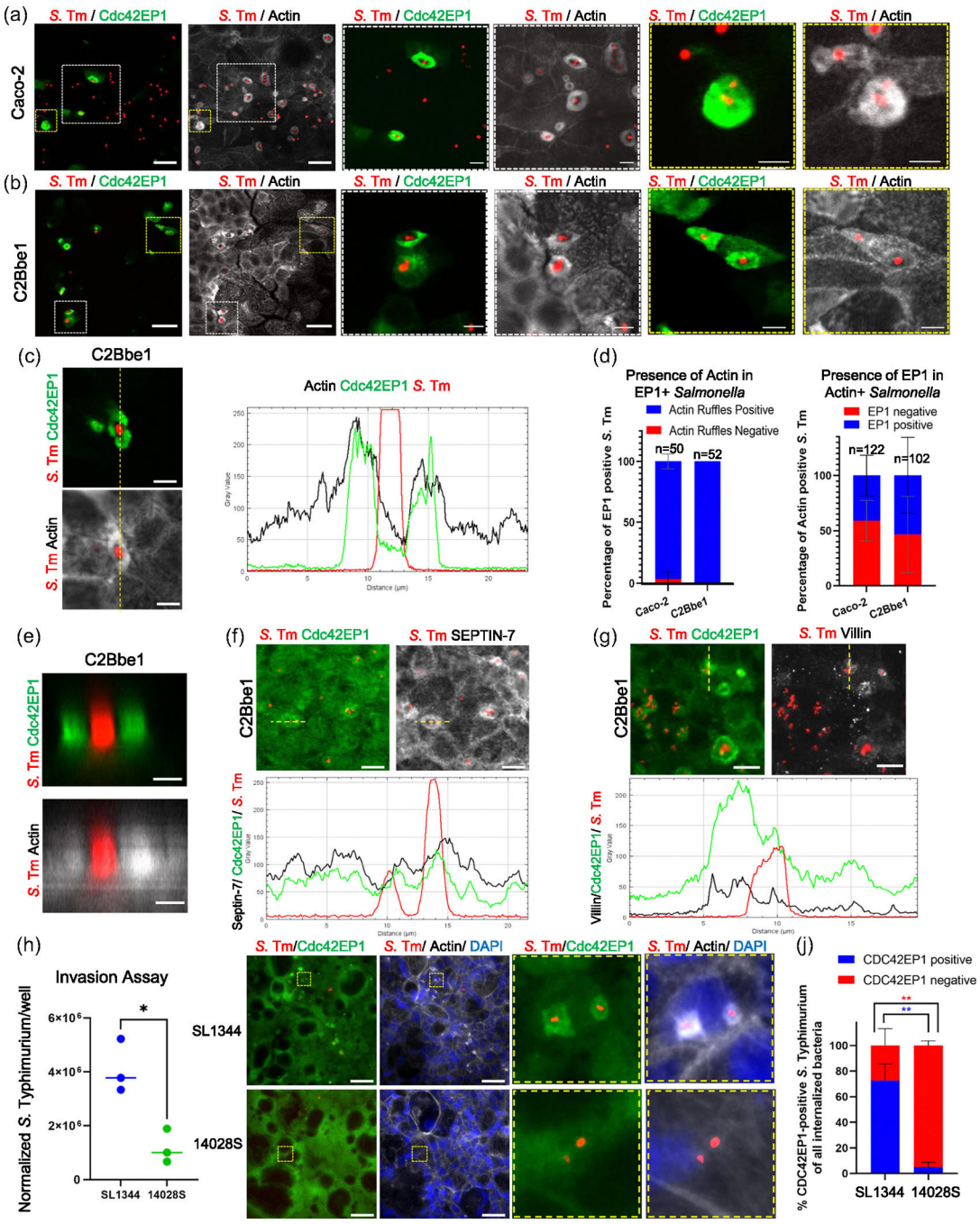


**FIGURE 3.**

Formation of an actin, septin, and villin-associated CDC42EP1 ring around invading *S.* Typhimurium requires CDC42 activation. (a, b) Immunostaining of *Salmonella* (red) and CDC42EP1 (green) in (a) Caco-2 and (b) C2Bbe1 cells 5 min after *S.* Typhimurium infection. Scale bars in lower magnification images (left) represent 20 μm. Scale bars for higher magnification micrographs of insets (right) represent 5 μm. (c) Line intensity profile of CDC42EP1, actin (phalloidin), and *Salmonella* from immunostaining in micrographs on left. Scale bar represents 5 μm. (d) Quantification of the percentage of invading *Salmonella*

in Caco-2 and C2Bbe1 cells that are surrounded by actin (phalloidin-positive) out of all invading *Salmonella* that are also surrounded by a CDC42EP1 ring (left); quantification of the percentage of invading *Salmonella* in Caco-2 and C2Bbe1 cells that are surrounded by a CDC42EP1 ring out of all invading *Salmonella* that are also surrounded by an actin bundle (right). (e) Side view (YZ) of cells in panel C. Note the relative height of CDC42EP1 and actin around the bacterium. Scale bars represent 3 μm. (f, g) Line intensity profile of CDC42EP1, *Salmonella*, and (f) SEPTIN-7 or (g) Villin from micrographs on top of 10 min *S*. Typhimurium infection in C2Bbe1 cells. Profile was obtained from intensities along yellow-dotted line. Scale bar represents 10 μm. (h) Gentamicin protection assay was employed to quantify *S*. Typhimurium colony-forming units (CFU) per well after a 30-min infection in C2Bbe1 cells infected with either SL1344 (WT *S*. Typhimurium) or 14028 S (GEF-deficient *S*. Typhimurium mutant). (i) Representative immunostaining of CDC42EP1 (green), actin (phalloidin; gray), *Salmonella* (red), and 4′,6-diamidino-2-phenylindole (DAPI) (blue) in C2Bbe1 cells infected with either SL1344 or 14028 S *S*. Typhimurium for 5 min. Scale bars in lower magnification images represent 50 μm. (j) Quantification of internalized SL1344 or 14028 S *S*. Typhimurium that are CDC42EP1-positive or CDC42EP1-negative.

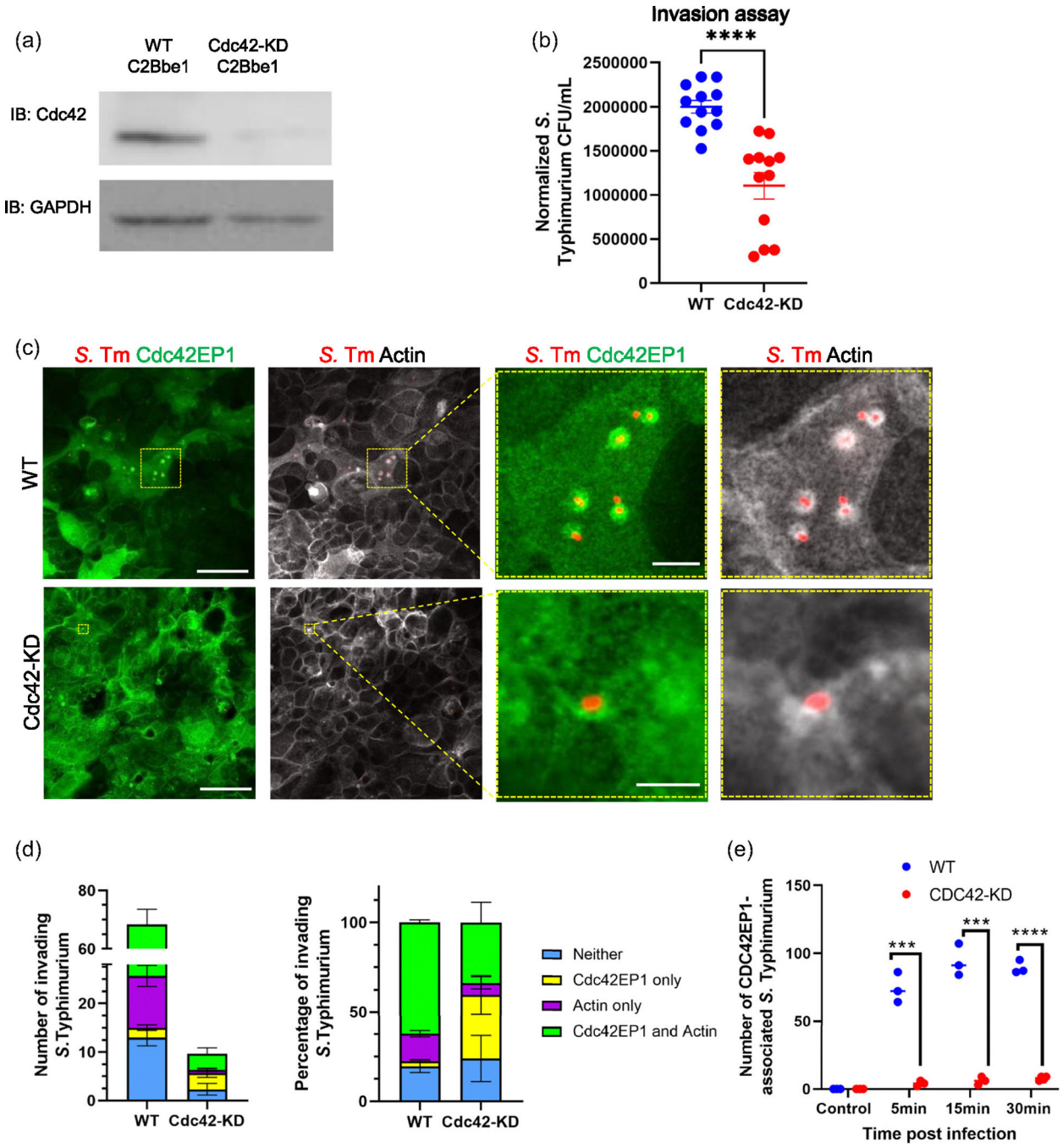


**FIGURE 4.**

CDC42 deficiency impairs CDC42EP1 recruitment to invasion sites and reduces *S.* Typhimurium invasion. (a) Immunoblot of WT and CDC42-KD C2Bbe1 cell lysates for CDC42 expression. (b) Normalized *S.* Typhimurium colony-forming units (CFU) counted after a 30 min *Salmonella* infection in WT and CDC42-KD C2Bbe1 cells using a gentamicin protection assay. (c) Representative immunostaining of *Salmonella* (red), CDC42EP1 (green), and actin (phalloidin; gray) after a 5-min *S.* Typhimurium infection in WT and CDC42-KD C2Bbe1 cells. Scale bar in lower magnification micrographs (left) represents 50

μm. Scale bar in high magnifications of insets for WT and CDC42-KD cells represent 10 and 5 μm, respectively. (d) Stacked bar graph showing the number (left) and percentage (right) of successfully invaded bacteria in WT or CDC42-KD C2Bbe1 cells that are surrounded by CDC42EP1 and actin enrichment (green), CDC42EP1 only (yellow), actin only (purple), or neither (blue). Bacteria were counted from three independent microscopic fields for each cell type. (e) Quantification of the number of CDC42EP1-associated internalized *S.* Typhimurium after each infection timepoint in WT (blue) and CDC42-KD (red) C2Bbe1 cells.

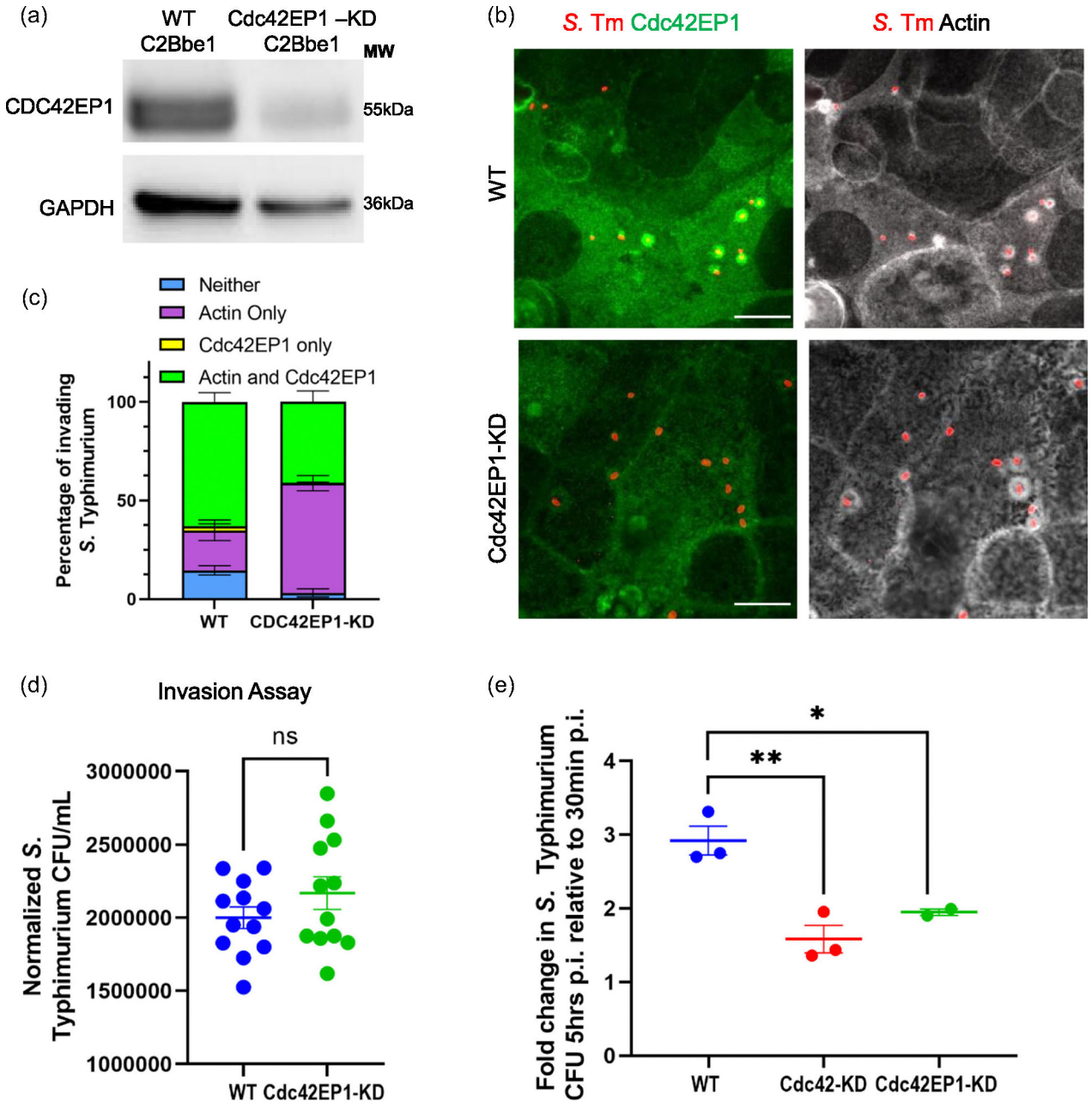


**FIGURE 5.**

CDC42EP1 deficiency impairs intracellular *S.* Typhimurium replication within host cells. (a) Immunoblot for CDC42EP1 using WT and CDC42EP1-KD C2Bbe1 cell lysates. (b) Representative immunostaining of *Salmonella* (red), CDC42EP1 (green), and actin (phalloidin; gray) after a 5-min *S.* Typhimurium infection in WT and CDC42EP1-KD C2Bbe1 cells. Scale bars represent 10 μm. (c) Stacked bar graph showing the percentage of successfully invaded bacteria in WT or CDC42EP1-KD C2Bbe1 cells that are surrounded by CDC42EP1 and actin enrichment (green), CDC42EP1 only (yellow), actin only (purple), or neither (blue). (d) Gentamicin protection assay was used to quantify colony-forming units (CFU) in WT and CDC42EP1-KD C2Bbe1 cells after a 30-min *Salmonella* infection. (e)

WT, CDC42-KD, and CDC42EP1-KD C2Bbe1 cells were infected for 30 min, washed out, and continued intracellular infection for 4.5 h. *S.* Typhimurium CFU was quantified from WT, CDC42-KD, and CDC42EP1-KD C2Bbe1 cells, and plotted as fold changes at 5 h time point relative to 30 min time point for each cell line. The results represent the intracellular growth of *S.* Typhimurium.